Journal of *Marine Science and Engineering*

MDPI

Article

Influence of Exit Setting Angle of Guide Vane on Bias Flow in Outlet Passage of Slanted Axial Flow Pump System

Lei Xu [1,*], Longcan Chen [1], Bo Zhu [1], Hucheng Zhang [2], Tao Jiang [1], Hongfei Duan [1] and Cheng Qian [1]

[1] College of Hydraulic Science and Engineering, Yangzhou University, Yangzhou 225009, China; longcanchenyzu@163.com (L.C.); zhubojsyzu@163.com (B.Z.); dx120210102@stu.yzu.edu.cn (T.J.); hongfei.duan@foxmail.com (H.D.); 18082062415@163.com (C.Q.)

[2] Yangzhou Survey Design Research Institute Co., Ltd., Yangzhou 225000, China; zhhch0905@163.com

* Correspondence: leixu@yzu.edu.cn

Abstract

A slanted axial-flow pump is extensively applied in coastal pumping stations; however, severe bias flow within the outlet passage will result in unstable operation and low efficiency of the slanted axial flow pump system. In order to mitigate bias flow in a slanted axial-flow pump outlet passage, seven exit setting angle schemes of the guide vanes were designed. The influence mechanisms of the guide vane exit setting angle on internal flow characteristics, hydraulic loss, flow deviation coefficient, vortex evolution patterns, and pump system efficiency were systematically investigated. The results demonstrate that under design flow conditions, as the exit setting angle of the guide vane ranges from 90° to 105°, the flow field in the first half of the guide vane remains essentially the same. The low-velocity region at the guide vane outlet demonstrates initial contraction followed by gradual expansion with increasing stagger angles. Looking downstream within the flow passage from the left to the right, the hydraulic loss in the outlet passage goes up after an initial descending trend as the exit setting angle increases. When the exit setting angle is 97.5°, the bias coefficient of the outlet passage is 1.031. At this point, the vortex core distribution intensity within the outlet passage reaches a minimum, corresponding to the lowest recorded hydraulic loss of 0.230 m. Compared with the original guide vane scheme, the scheme with an angle set at 97.5° can improve the pump system efficiency of the slanted axial flow pump system, whether the flow is set at a design point or at a large point, and the pump system efficiency is increased by 2.3% under design flow conditions.

Keywords: slanted axial flow pump system; outlet passage; bias flow; guide vane; numerical simulation

check for updates

Academic Editor: Alon Gany

Received: 29 June 2025
Revised: 19 July 2025
Accepted: 22 July 2025
Published: 24 July 2025

Citation: Xu, L.; Chen, L.; Zhu, B.; Zhang, H.; Jiang, T.; Duan, H.; Qian, C. Influence of Exit Setting Angle of Guide Vane on Bias Flow in Outlet Passage of Slanted Axial Flow Pump System. *J. Mar. Sci. Eng.* **2025**, *13*, 1413. https://doi.org/10.3390/jmse13081413

Copyright: © 2025 by the authors. Licensee MDPI, Basel, Switzerland. This article is an open access article distributed under the terms and conditions of the Creative Commons Attribution (CC BY) license (https://creativecommons.org/licenses/by/4.0/).

1. Introduction

Among the main types of low-lift pumping stations, the slanted axial-flow pump system has the advantages of economical civil engineering, good hydraulic performance, good heat dissipation conditions, and convenient maintenance [1,2]. The first inclined-shaft Kaplan pump was used in Wagboden, Austria, in 1962. The slanted axial flow pumps are widely used in Egypt, inclined-shaft Kaplan pumps with electro-mechanical drives for adjustable impeller blades for irrigation were used in EI Slalam 1-3 Egypt in 1992, modernization of six inclined axial pumps for drainage of waste water were used in EI Max Egypt in 1996, and modernization of four inclined axial pumps for drainage were used in Kassaby Egypt in 2003 [2]. The earliest slanted shaft extension pumping station built is the Honggebo Pumping Station in Inner Mongolia, China, and the inclination angle of the

pump shaft is 45°. Subsequently, slanted axial-flow pump systems using 15°, 20°, 30°, and 45° shaft inclination angles have been successfully applied in water conservancy projects in regions such as Shanghai, Zhejiang, and Guangdong [3–6]. Scholars have implemented comprehensive hydrodynamic evaluations of pump systems with 30° shaft inclination angles, focusing on operational performance, entire flow passage optimization [7–10], and model-based predictions of their real-world performance [11]. The slanted axial flow pump system comprises the inlet passage, impeller chamber, guide vane, and outlet passage, and its hydraulic performance depends on these four components and their interactions. Scholars have found that there is a tendency for unequal flow between bifurcated outlet passages in the slanted axial-flow pump system, which has detrimental effects on the hydraulic efficiency and operational stability of the whole system, and even affects the stable operation of the small flap gates on the working gates at the exit of the outlet passage [12]. At the same time, it will lead to high energy consumption and low efficiency of the slanted axial flow pump system.

Some experts and scholars have studied the hydraulic performance of the slanted axial flow pump system. Chen et al. [13] studied the energy characteristics of the slanted axial flow pump under various wall roughnesses. He et al. [14] tested a model pump system with a shaft inclination angle of 15° optimized by numerical simulation; the results showed that the pump system had superior performance. Xie et al. [15] conducted a hydrodynamic experiment test on the new 15° slanted axial-flow pump system of Yanguan Pumping Station in Zhejiang Province, and found that the cavitation characteristics of the pump system at small blade angles were better than those of large blade angles. Tong et al. [16] used a hybrid optimization method based on entropy dissipation to study the hydraulic performance of a slanted axial-flow pump. The results showed that the preferred working range was expanded when using this method, and the head and efficiency of the pump were also significantly improved. Fei et al. [17] studied the hydraulic performance and tip leakage vortex of a slanted axial flow pump under different blade angles by the CFD method. The results revealed that as the blade angle grows larger, the pump head and the flow rate at best efficiency both increase.

The hydraulic performance of the slanted axial flow pump system is excellent, but there is a tendency for flow deviation in the outlet passage, and some scholars have also carried out research on this. Lu et al. [18] used a 3D numerical simulation method to study the flow morphology of the slanted outlet passage, and found that there were different degrees of vortices near the outlet section, which was consistent with the model test results. In order to solve the problem of deflection of the outlet passage in the slanted pump system, Xu et al. [19] studied a 20° slanted shaft extension pump system through numerical simulation, and found that the bias in the slanted outlet passage was severe. They analyzed the causes of the flow deviation and proposed a solution to extend the length of the middle pier in the outlet passage. As the length of the middle pier increased, the volume flow rate of the left and right holes of the outlet passage gradually became almost equal. Xu et al. [20] also studied the influence of the guide plates installed in the curved section on the hydraulic performance of the slanted outlet passage; the guide plate measurements were used to solve the bias flow problem. Wang et al. [21] studied the transient flow inside the slanted axial flow pump system model of Yanguan Pumping Station in Zhejiang Province by means of model tests and numerical analysis. The cause of bias flow was analyzed, and a method was proposed to set inhibition measures in the elbow section of the outlet passage to improve the bias flow. Numerical simulation analysis and model test were conducted on a certain slanted pump device by Yan [22]. The calculation showed that there was a serious flow bias problem in the slanted outlet passage. The essence of the deviation problem was analyzed as being caused by the spiral flow with circulation entering the slanted outflow

channel, and the method of setting the deflector in the inlet bending section of the outflow channel and changing the length of the middle partition pier was proposed to solve the bias flow problem of the slanted outflow channel.

In the slanted pump system, the outlet passage is located behind the guide vane, and the water flowing from the guide vanes still has substantial residual circulation movement [12]. The non-uniform flow distribution within the outlet passage arises due to the combined influence of circulation and the curvature of the passage. Different from the existing measures, such as adding guide plates in the inlet bending section of the slanted outlet passage and increasing the length of the middle partition pier, the exit setting angle of the guide vane is considered in this paper. When the exit setting angle of the guide vane is not suitable for the outlet passage, the problem of bias flow and vortex will occur in outlet passage, and further leads to low efficiency and severe vibration of the pump system. Thus, different exit setting angle schemes are designed based on a slanted axial-flow pump system (shaft angle: 20°). By the method of numerical simulation, the bias flow, hydraulic loss in the outlet passage, flow patterns, and changes in vortex structures under different schemes are calculated and analyzed, in order to solve the bias flow problem in the outlet passage.

2. Numerical Simulations and Research Schemes

2.1. Numerical Simulations

2.1.1. Governing Equations and Turbulence Model

The water flow within the slanted axial-flow pump system exhibits continuous and incompressible characteristics, and energy is imparted to the water as it passes through the impeller chamber. Numerical simulations employing the Reynolds-averaged Navier–Stokes Equations [23,24] with the standard k-ε turbulence model demonstrate enhanced congruence with flow patterns in the slanted axial-flow pump system. The selected turbulence closure combines structural simplicity with convergence stability, effectively resolving high-Reynolds-number turbulent flow characteristics within pump passages [22]. This validated modeling approach provides reliable predictions of both field and hydraulic performance of the slanted axial flow pump system.

The Reynolds-averaged transport equations governing turbulent kinetic energy (k) and turbulent dissipation rate (ε) in the standard k-ε turbulence model can be expressed as follows:

k equation:

$$\frac{\partial(\rho k)}{\partial t} + \frac{\partial\left(\rho k\overline{u'_i}\right)}{\partial x_i} = \frac{\partial}{\partial x_j}\left[\left(\mu + \frac{\mu_t}{\sigma_k}\right)\frac{\partial k}{\partial x_j}\right] + G_k - \rho\varepsilon + S_k \tag{1}$$

ε equation:

$$\frac{\partial(\rho\varepsilon)}{\partial t} + \frac{\partial\left(\rho\varepsilon\overline{u'_i}\right)}{\partial x_i} = \frac{\partial}{\partial x_j}\left[\left(\mu + \frac{\mu_t}{\sigma_\varepsilon}\right)\frac{\partial \varepsilon}{\partial x_j}\right] + C_{1\varepsilon}\frac{\varepsilon}{k}G_k - C_{2\varepsilon}\rho\frac{\varepsilon^2}{k} + S_\varepsilon \tag{2}$$

where ρ is the fluid density. k is the turbulent kinetic energy. t is the time. $\overline{u'_i}$ is the time-averaged velocity component. x_i and x_j are the coordinate components. μ is the laminar viscosity coefficient. μ_t is the turbulent viscosity coefficient. $C_{1\varepsilon}$, $C_{2\varepsilon}$, C_μ, σ_k, and σ_ε are the model constants. G_k is the generation term of turbulent kinetic energy k due to the average velocity gradient. ε is the turbulent viscosity coefficient.

The recommended values of Launder et al. and the results of later experimental validation were used in the standard k-ε turbulence model [25], $C_{1\varepsilon}$, $C_{2\varepsilon}$, C_μ, σ_k, and σ_ε were taken as $C_{1\varepsilon} = 1.44$, $C_{2\varepsilon} = 1.92$, $C_\mu = 0.09$, $\sigma_k = 1.0$, and $\sigma_\varepsilon = 1.3$.

2.1.2. Calculation Parameters and Boundary Conditions

A shaft-inclined axial flow pump with a shaft inclination angle of 20° is chosen for research. The calculation domain of the model includes four parts, and the CFD model is shown in Figure 1. Moreover, the main parameters are listed in Table 1.

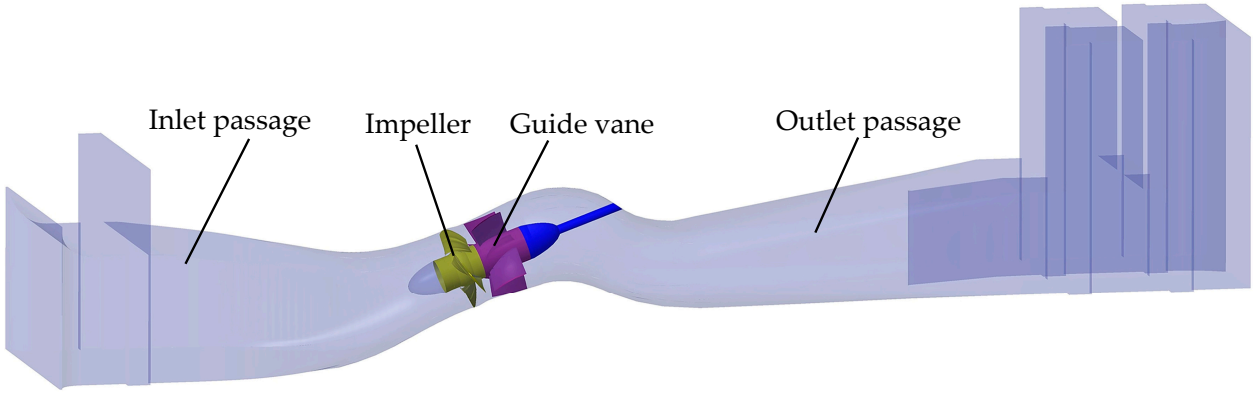


Figure 1. Three-dimensional model of numerical calculation of slanted axial flow pump system.

Table 1. Main parameters of the slanted axial flow pump system.

Parameters	Value
Design discharge rate	45 m^3/s
Rotating speed	107.1 r/min
Impeller diameter	3.65 m
Number of impeller blades	4
Number of guide vanes	7
Blade angle of impeller	−4°
Inclination angle of pump shaft	20°

Table 2 shows the boundary condition settings for the computational domain of the pump system. It includes boundary conditions such as velocity-inlet, outflow, and so on.

Table 2. Boundary condition settings of the pump system.

Location	Boundary Condition
Inlet	Velocity-inlet
Outlet	Outflow
Solid wall	No-slip wall
Free water	Symmetry
Convergence accuracy	10^{-6}

2.1.3. Mesh Generation

An unstructured tetrahedral mesh was used to mesh sections shown in Figure 1 due to the complex geometry of the pump system, and a hexahedral structured mesh was used for the extension parts. The meshing result is shown in Figure 2.

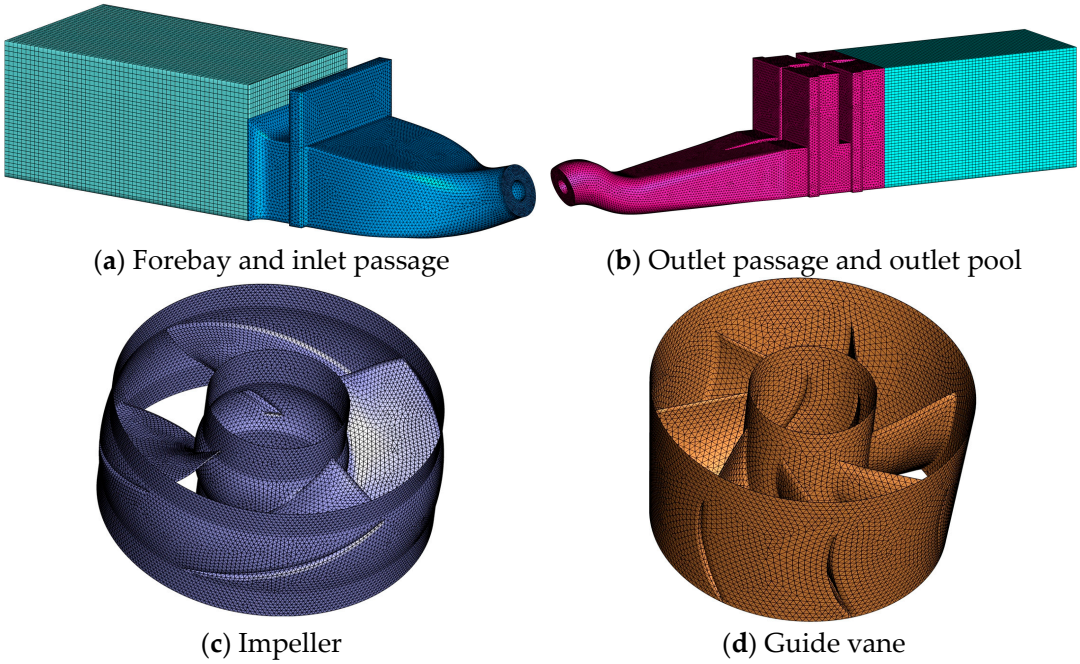


Figure 2. Meshing of the pump system.

2.1.4. Grid Independence Verification

This study conducts a grid independence analysis for the numerical simulations of the inclined pump system. Figure 3 illustrates the effect of varying grid sizes on the efficiency of the pump system.

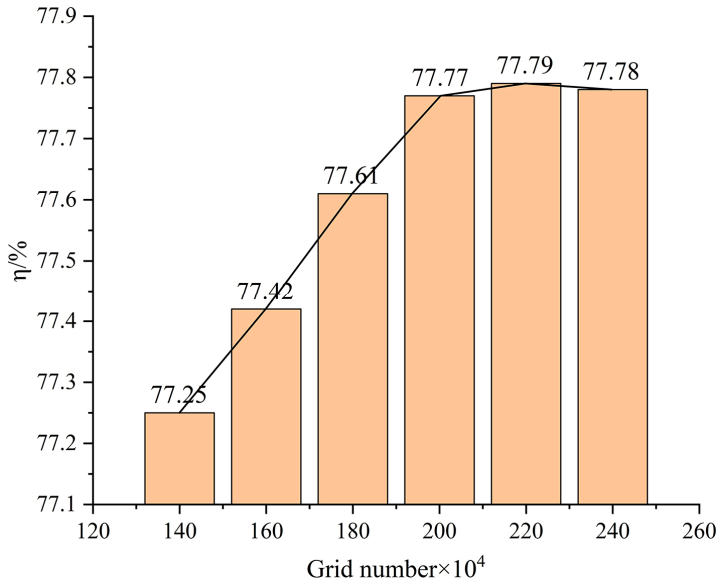


Figure 3. Grid independence analysis of the slanted pump system.

As illustrated in Figure 3, a significant efficiency improvement appeared when the mesh density increased from 1.4 million to 2.0 million. However, further mesh refinement yielded negligible efficiency variation (<0.2% deviation), thereby satisfying the convergence criteria [26]. Consequently, the final computational mesh configuration was determined as 2,000,000 grid elements.

2.1.5. Verification of Numerical Simulation Results

To validate the reliability of the numerical simulation method for the pump system proposed in this study, the proposed method was applied to simulate the energy performance of the slanted axial-flow pump system at Baobao Pumping Station under the blade angle of −4° [27]. The flow calculation range is from 35 m^3/s to 50 m^3/s. The model test was completed on the hydraulic machinery test bench of Bei Fang Investigation, Design & Research Co., Ltd., Tianjin, China. The stability and accuracy of the test bench are excellent; the comprehensive uncertainty error of efficiency is less than 0.3%, and the random error is less than 0.1% [28]. Based on the pump system model test report of the Baibao Pumping Station, the comprehensive uncertainty of the energy performance test for the pump system is ±0.26%. According to the similarity criterion between the prototype and the model, when the impeller blade is placed at an angle of −4°, the measured results from the model tests are scaled to obtain the energy performance curve of the prototype pump. Figure 4 compares the numerical simulation results with the model test data regarding the energy performance of the pump system, where η_{zz} is the efficiency of the pump system.

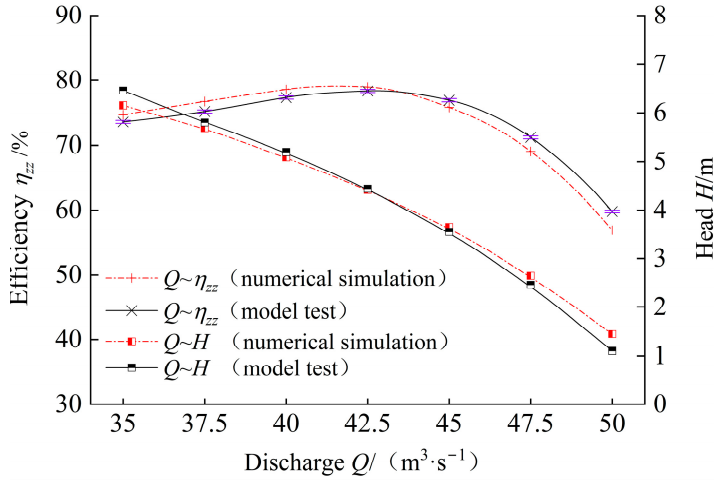


Figure 4. Comparison of numerical simulation and model test results of energy performance of Babao Pumping Station.

At the design flow rate, the model test efficiency of the pump was measured as 76.90%, and the head was 3.55 m. The results obtained by numerical simulation are as follows: the efficiency is 75.83%, and the head is 3.65 m. After comparison, it can be found that under the design condition, the numerical simulation and model test results show a 1.07% difference in efficiency and a 0.1 m discrepancy in head. The calculation error of the pump system efficiency at the optimal operating condition is 0.79%. In addition, under other operating conditions, the differences are small and within the allowable error range. The results demonstrate that the numerical simulation method adopted in this study is reliable and capable of accurately simulating the internal flow characteristics within the outlet passage.

2.2. Schemes of Exit Setting Angle of Guide Vane

The guide vanes facilitate energy conversion by transforming the kinetic energy associated with the impeller's circumferential velocity into pressure energy. This process achieves three critical objectives: circulation recycle, hydraulic loss mitigation, and efficiency enhancement. Figure 5 shows the structural parameters of the guide vane. The exit setting angle (β in Figure 5) is an important design parameter of the guide vane. Changing the exit setting angle can adjust the rotation angle of the water flow out of the guide vane near the vane outlet [22,29,30], altering the circulation of the water flow, so as to address the problem of flow deviation [31], which offers a new perspective for improving the deviation

flow issue in the outlet passage of analogous pump systems. The combined effects of residual inertial forces in the flow exiting the guide vanes and the blade blockage effect caused by the finite number of vanes result in the flow angle at the guide vane exit being smaller than the exit setting angle, creating a measurable flow deviation angle. There is a certain angular deviation between the guide vane flow angle and the exit setting angle of the guide vane. Theoretically, increasing the exit setting angle will ensure that the guide vane flow angle is 90°, which guarantees that the water flow exiting the guide vane outlet has no circulation [32].

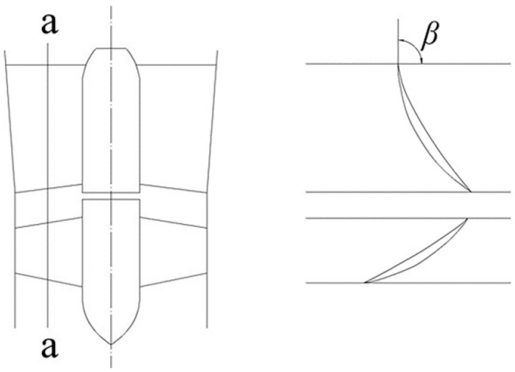


Figure 5. Structure parameter diagram of guide vane.

Therefore, based on the original exit setting angle, while keeping the length and number of guide vanes unchanged, this paper gradually changes the exit setting angle within the range of 90.0° to 105.0°, forming five calculation schemes for the exit setting angle of guide vanes. This paper mainly analyzes the following five schemes: β = 90.0°, β = 95.0°, β = 97.5°, β = 100.0° and β = 105.0°. The bias flow coefficient, total head loss, and pump system efficiency were used as the hydraulic performance evaluation indices, and the bias flow coefficient λ of the outlet passage was the most critical index. Perspective views of the pump section with five representative exit setting angles, along with comparative diagrams of the guide vane geometries, are illustrated in Figures 6 and 7, respectively.

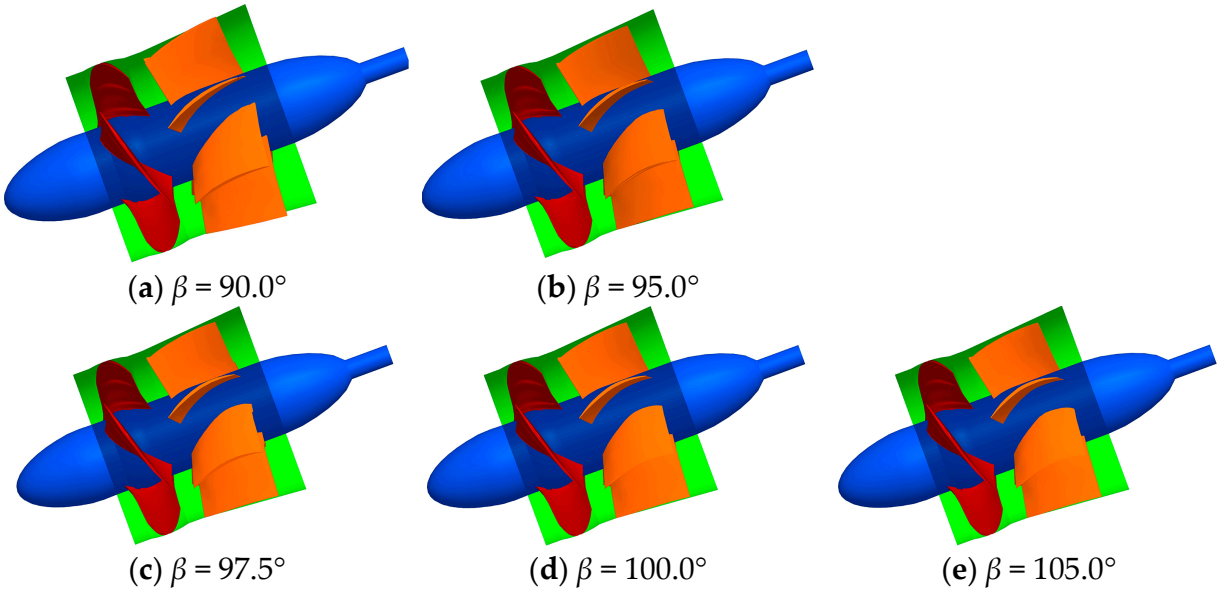


Figure 6. Perspective view of the pump section for different schemes.

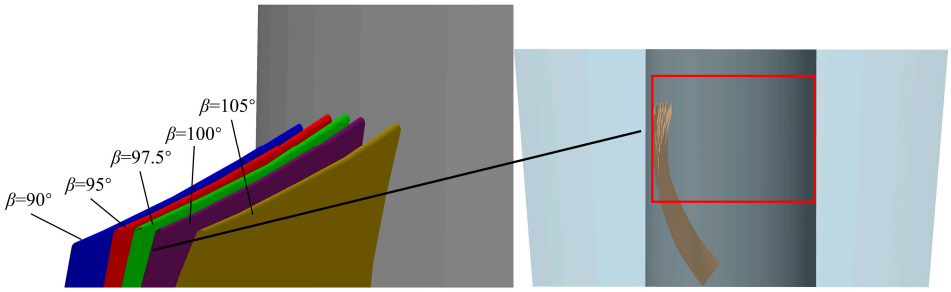


Figure 7. Comparison of guide vane models.

Designing an appropriate guide vane exit setting angle to ensure equal flow in both outlet passages, maximize the recovery of circulation by the guide vanes, improve the efficiency of the whole pump system, and minimize the hydraulic loss of the guide vanes and the outlet passage are the main research objectives of this paper.

3. Results and Analysis

3.1. Hydraulic Performance Comparison of Different Guide Vane Schemes

The deviation flow within the outlet passage is characterized by different flow rates on either side of the middle dividing pier. To clearly judge the deviation flow situation, the bias flow coefficient is introduced to characterize the deviation flow. When λ is greater than 1, it indicates a higher flow rate through the left hole compared to the right one, whereas λ below 1 signifies the opposite. The closer λ is to 1, the smaller the degree of deviation of the flow is. The specific formula is as follows:

$$\lambda = \frac{Q_{left}}{Q_{right}} = \frac{A_{left}\overline{v}_{left}}{A_{right}\overline{v}_{right}} \tag{3}$$

where Q_{left} and Q_{right} are the volume flow rates through the left and right holes of the outlet passage, m^3/s. A_{left} and A_{right} are the sectional areas of the holes on the two sides, m^2. $\overline{v}_{left}$ and $\overline{v}right$ are the average flow velocities of the sectional area of holes on two sides, respectively, m/s.

Figure 8 presents a comparison of the bias flow coefficients under different exit setting angle schemes at the design flow rate. As the angle increases, the coefficient decreases gradually, and the change in amplitude is fast at first and then slow. The exit setting angle is approximately demarcated at 97.5°, with the bias flow coefficient of 1.031 at this angle, indicating that the deviation flow issue has been essentially resolved. When the angle is less than 97.5°, λ is greater than 1. As the angle becomes smaller, λ demonstrates an inverse trend. When the angle is greater than 97.5°, the bias flow coefficient drops below 1.

The hydraulic losses within the passage are calculated by measuring the total pressure difference between two sections. The specific formula is as follows:

$$h = \frac{P_2^T - P_1^T}{\rho g} \tag{4}$$

where h is the hydraulic loss, m. ${P_2}^T$ and ${P_1}^T$ represent the total pressure of the measured section, Pa. g is the acceleration due to gravity, m/s^2. ρ is the density of water, kg/m^3.

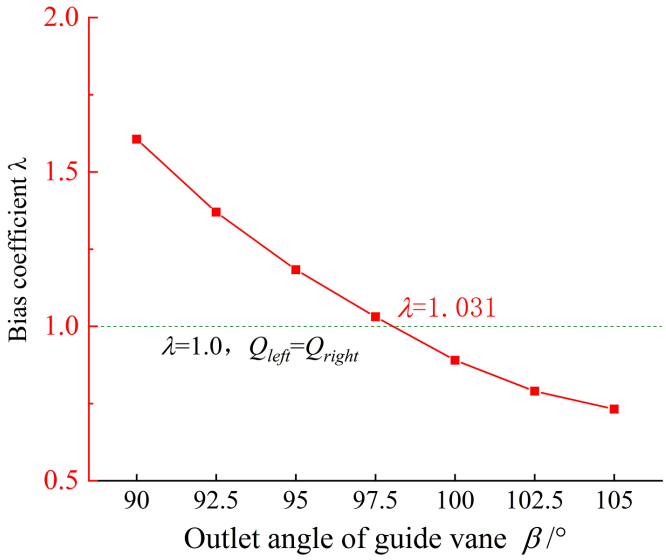


Figure 8. Bias coefficient for different schemes.

Figure 9 illustrates the variation in hydraulic losses of the guide vane and the outlet passage under different schemes, where the green line represents the losses of the outlet passage and the blue line represents the losses of the guide vane body. As illustrated in Figure 9, the hydraulic losses in the guide vane assembly increase progressively with larger outlet angles, while the hydraulic losses within the discharge passage exhibit a concave trend—initially decreasing and subsequently increasing—as the outlet angle rises. When the exit setting angle is 97.5°, the minimum loss of the outlet passage is 0.230 m. In addition, $\Delta h_{passage}$ changes little when the exit setting angle is between 97.5° and 100°. When the exit setting angle exceeds the above range, $\Delta h_{passage}$ will increase dramatically.

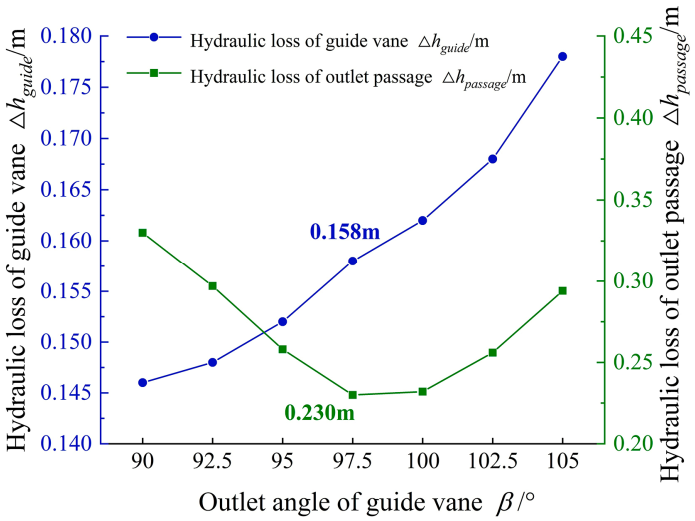


Figure 9. Hydraulic loss of guide vanes and outlet passage.

Combined with the bias flow coefficient, it can be found that when β = 97.5°, the hydraulic loss of the outlet passage reaches its minimum value and the flow rate in two holes is basically equal, it shows that choosing the appropriate exit setting angle can indeed solve the problem of deflection in the outlet passage of the slanted axial-flow pump system. If the outlet angle of the guide vanes is not chosen appropriately, not only will the hydraulic loss of the guide vanes increase, but the hydraulic loss of the outlet passage will also increase.

To address the problem of flow bias in the outlet passage of the slanted pump system, an alternative measure, which is to add a guide plate in the curved section of the outlet passage, has been studied [20]. Compared with this measure, the measure adopted in this paper, which is to change the outlet angle of the guide blade, has the following advantages: (1) No additional guide plates are needed, only the outlet angle of the guide blade needs to be changed; (2) It is beneficial to reduce the hydraulic loss of the outlet passage, while the hydraulic loss of the outlet passage will increase with adding guide plate in the curved section; (3) It does not increase the construction difficulty, adding guide plate will increase the manufacturing workload and is not convenient for construction; (4) It does not increase the operation and management difficulty, for the guide plate measure, it is easy to accumulate attachments on the guide plate and needs to be cleaned frequently after long-term operation.

3.2. Internal Characteristic Comparison of Different Guide Vane Schemes

When β is set at 97.5°, λ basically equals 1. Five schemes were selected with guide vane exit setting angles of 90°, 95°, 97.5°, 100°, and 105°. Under design flow rate conditions, the flow field of the guide vane and the outlet passage under five different exit setting angles was analyzed.

Figure 10 presents the velocity cloud diagram of the guide vane at different exit setting angles and spans. In the figure, the red circles are used to highlight the contrast in the flow field distribution at the same position. As illustrated in Figure 10, the flow velocity within the airfoil-shaped passages of the guide vane is basically the same under different exit setting angle schemes, generally showing a trend of higher velocity at the inlet and lower velocity at the outlet. When the span is 0.1, localized low-velocity zones are observed near the leading edge region of the guide vane inlet. The low-velocity zone area adjacent to the guide vane inlet exhibits a concave trend, first decreasing and subsequently increasing with the augmentation of the exit setting angle. The local minimum is achieved at 97.5°.

When the span is 0.5, localized flow separation is observed near the guide vane trailing edge, with the recirculation zone area progressively diminishing as the exit setting angle increases. When the span is 0.9, flow separation occurs near the guide vane trailing edge, similar to the case at span 0.5; however, the recirculation zone area near the trailing edge demonstrates a progressively increasing trend with larger exit setting angle. As evidenced by the preceding analysis, the internal flow within the guide vane exhibits significant complexity. Low-velocity zones near the hub predominantly manifest at the guide vane inlet region, while those adjacent to the shroud are primarily concentrated near the trailing edge. In general, the reflux area of the scheme with the exit setting angle of 97.5° is smaller than that of other schemes. If the outlet angle of the guide vane is improperly designed, it will cause vortices to form on the back of the guide vane, thereby affecting the stability of water flow.

Figure 11 presents the pressure cloud diagrams of the guide vane under different schemes. The pressure tends to be lower at the inlet and higher at the outlet, which corresponds to the velocity cloud diagrams. The scheme of the angle set at 90° demonstrates lower overall pressure within the guide vane compared to other schemes, while achieving a more uniform pressure distribution at the outlet. The pressure contours of the angle of 95° and 97.5° schemes are similar. Higher pressure is observed on the pressure side compared to the suction side of the guide vane blades. The pressure on the pressure surface of each guide vane blade is basically the same and evenly distributed. A pressure reduction is observed on the pressure side of the guide vane blades near the hub region of the guide vane inlet, accompanied by marginally lower flow velocity in this specific area compared to adjacent sections. When the pressure at the inlet of the guide vanes drops to a certain level,

cavitation will occur, and subsequently, erosion by cavitation takes place. For the guide vane of an axial flow pump, near the optimal operating condition, the guide vanes match well with the water flow at the outlet of the impeller, and the water flow velocity is not high, so cavitation does not usually occur. However, for non-design operating conditions, especially the large flow conditions deviating from the efficient zone, the flow state at the inlet of the guide vanes is poor, and the flow velocity increases significantly, making cavitation prone to occur. Therefore, attention needs to be paid to the changes in the inlet pressure of the guide vanes during non-design operating conditions. For the other two schemes, the pressure contour diagram of the guide vane reveals a non-uniform pressure distribution at the shroud exit region, which predisposes this area to flow separation phenomena, a conclusion corroborated by the velocity contour analysis.

On the whole, the pressure distribution across the guide vane blades, shroud, and hub regions exhibits significant non-uniformity, which induces localized flow separation phenomena at both the inlet and outlet of the guide vane, and the flow pattern is chaotic.

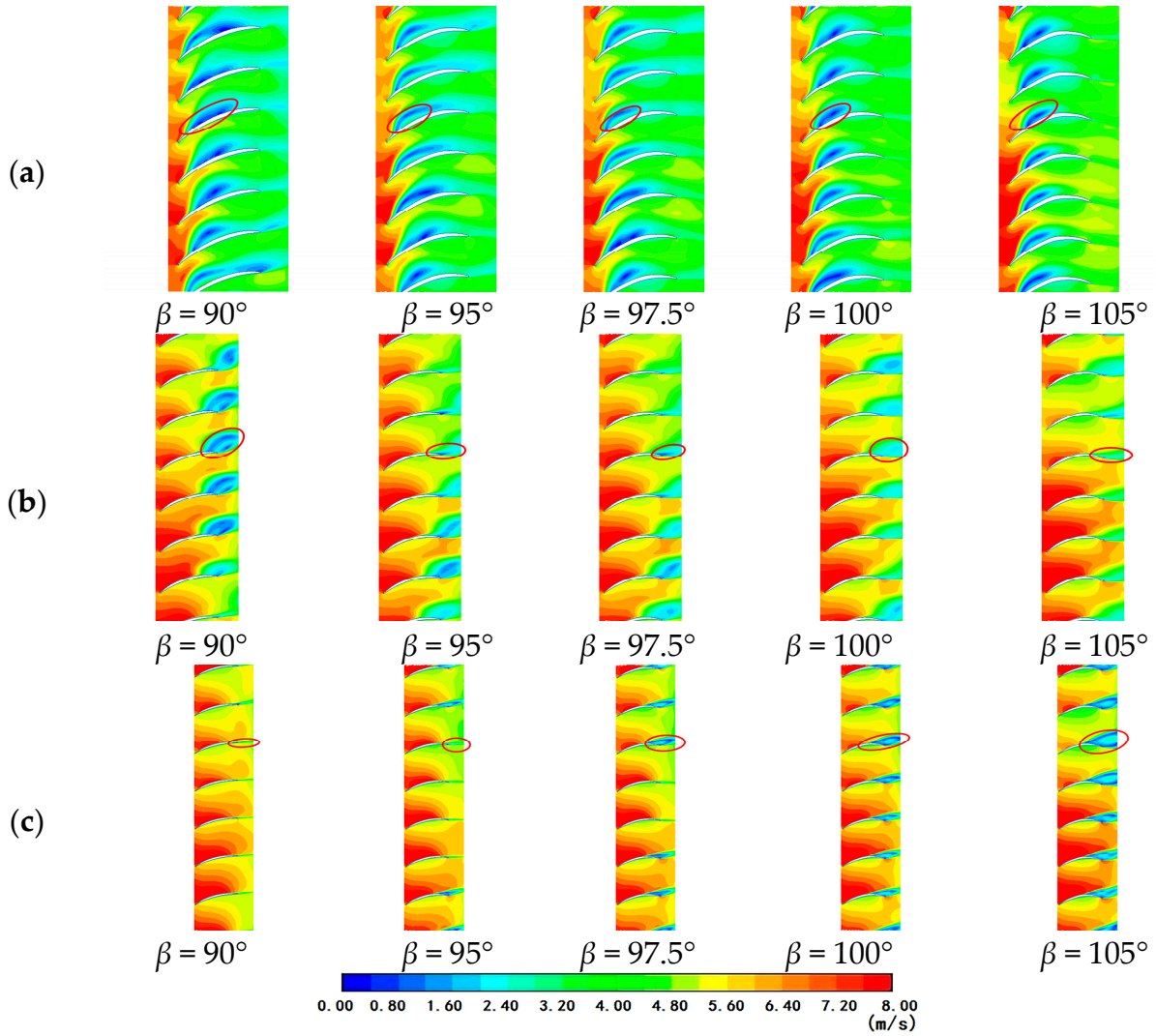


Figure 10. Velocity cloud of the guide vane at different exit setting angles and spans. (**a**) span = 0.1, (**b**) span = 0.5, and (**c**) span = 0.9.

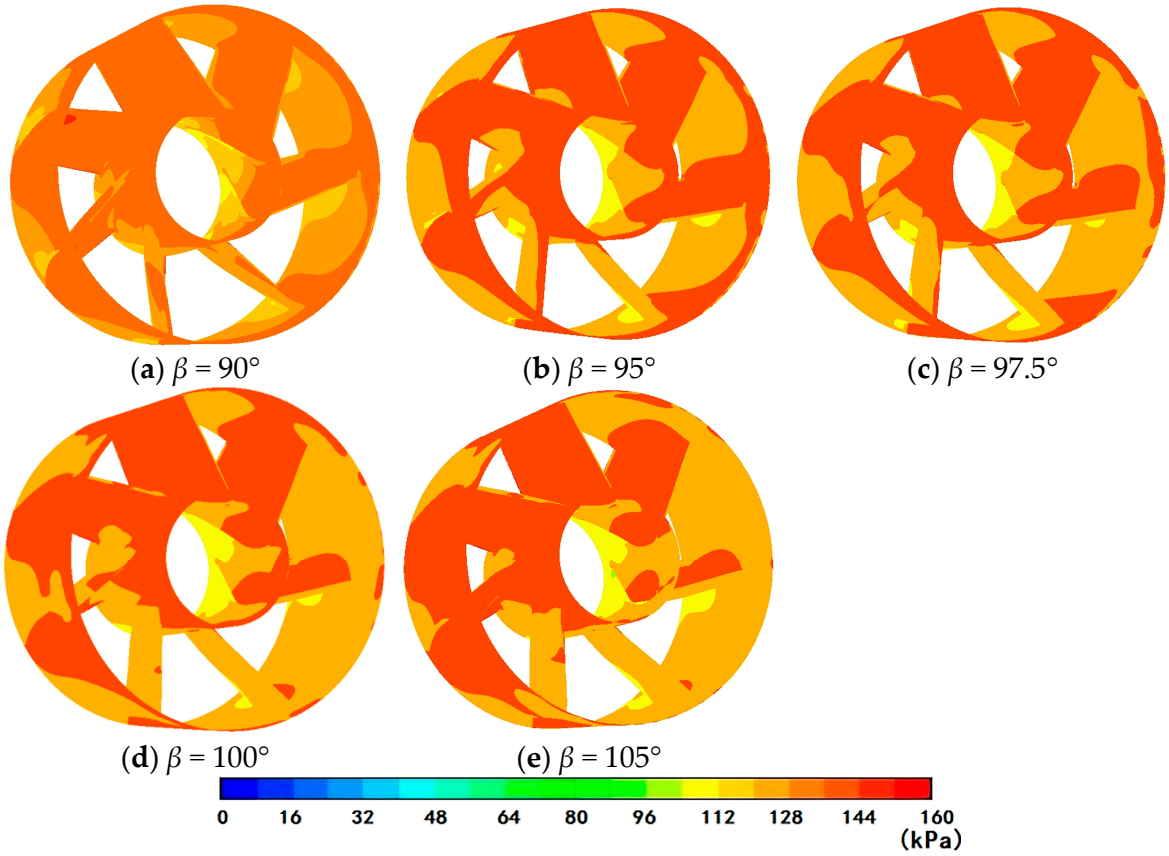


Figure 11. Cloud chart of guide vane sidewall pressure under different schemes.

Figure 12 shows the internal water flow streamline patterns in the outlet passage under different exit setting angle schemes. When water passes through the pump impeller, it acquires energy from the impeller's rotation and then flows into the guide vane, where the water is redirected. When viewed along the flow direction, the water enters the outlet passage while exhibiting counterclockwise rotational motion. Pathline visualizations reveal significant flow asymmetry in the outlet passage when employing the exit setting angles of 90° and 95°, with left-side streamline velocities exceeding right-side counterparts. Additionally, a large-scale vortex structure persists in the right anterior region of the middle pier, indicating a low-velocity zone in this section, which also leads to reduced flow rate on the right side and a flow deviation coefficient greater than 1. When the angle is 97.5°, there is a small and symmetrical vortex in the front side of the pier, and the flow velocity on the two sides of the passage is basically the same. As the angle increases further, the vortex begins to shift to the left. The larger the exit setting angle is, the wider the range of the vortex is. Consequently, the right-side flow velocity now exceeds the left-side, resulting in the bias flow coefficient below 1. When the exit angle of guide vane is far away from 97.5°, the vortex zone in the front side of the pier will become larger and be close to one side of the outlet passage, as a result, it leads to bias flow in outlet passage, the hydraulic loss of outlet passage will become larger, and the efficiency of pump system will be decreased.

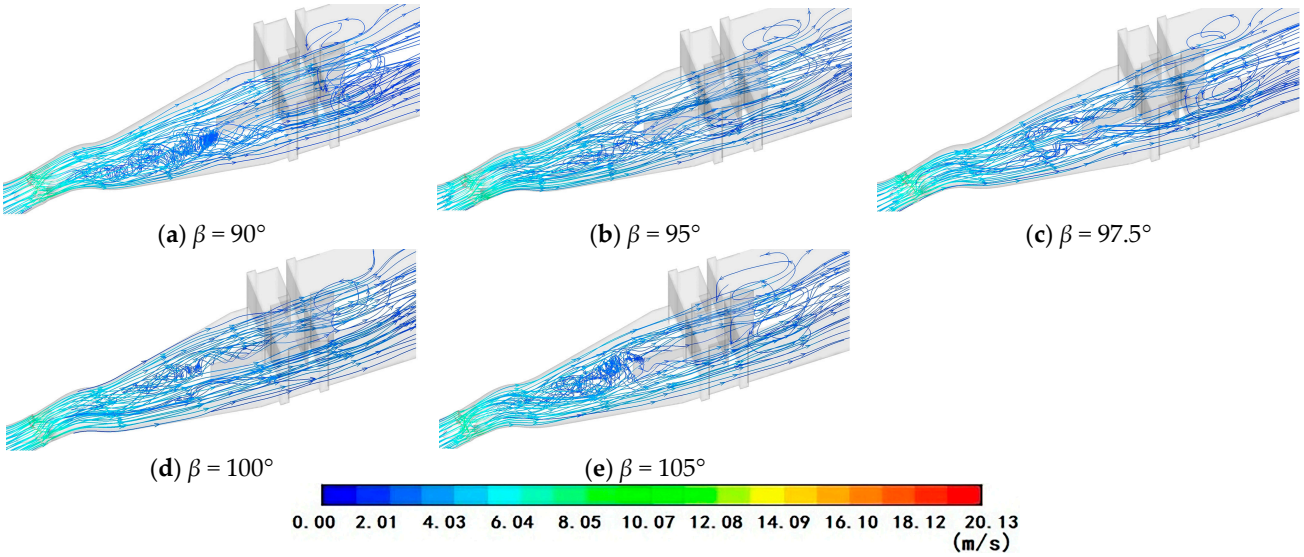


Figure 12. Streamline patterns in the outlet passage under different exit setting angle schemes.

Figure 13 is the velocity distribution diagram of the selected characteristic sections in the outlet passage. Cross-sectional velocity profiles demonstrate that all schemes exhibit similar flow velocity distributions at the guide vane outlet section, with each section showing the characteristic of lower velocities at the center and higher velocities at the periphery. After passing through the bending section at the front of the outlet passage, the flow regime of each scheme is different. At an angle of 90°, the majority of the water flow is located at the upper left side. As the angle increases, the main stream first moves to the middle and upper part, then to the upper right side, and finally, when the exit setting angle is 105°, the main stream of the passage is concentrated on the right side. In the straight diffusion section after the bending section, the low-speed rotating water flow further develops and expands. When the angle is 97.5°, the rotating low-velocity water flow gradually evolves into two symmetrical streams, with opposite rotation directions.

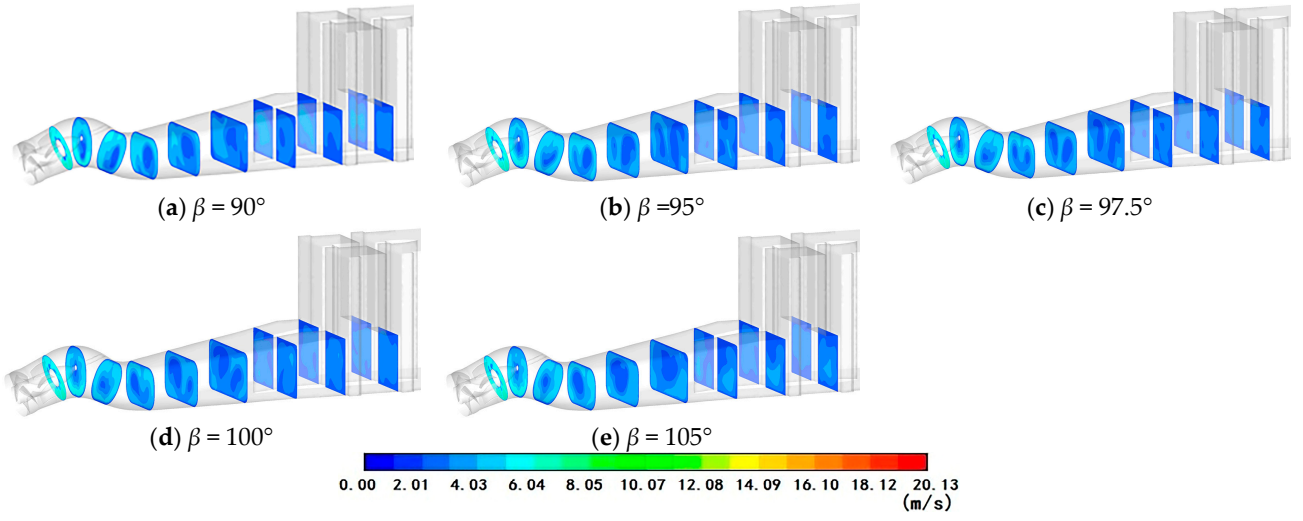


Figure 13. Flow velocity distribution of a typical cross-section.

The results show that when the angle is 97.5°, the internal flow pattern of the outlet passage is relatively symmetrical, with the flow rates in the left and right openings being essentially the same, which can improve the bias flow problem in the discharge channel of the inclined pump device.

3.3. Analysis of the Vortex Structure in the Outlet Passage

Vortex structures within the discharge passage were analyzed using the third-generation vortex identification method (the Omega criterion) [33], with isosurface visualization color-mapped by velocity magnitude (v). Compared to traditional methods that require adjusting the threshold value over a large range, the Ω criterion has the advantage of normalizing threshold values. The Ω criterion threshold is normalized to between 0 and 1; furthermore, the Ω criterion demonstrates superior capability in detecting weak vortex structures. The general recommendation is to use a value of Ω = 0.52 for the isosurface representation of vortices. The core identification parameter formulas of the Ω criterion are similar to the traditional Q criterion, as follows:

$$\Omega = \frac{\|\omega\|_F^2}{\|D\|_F^2 + \|\omega\|_F^2 + \varepsilon} \tag{5}$$

$$\varepsilon = 0.001 \times \left(\|D\|_F^2 - \|\omega\|_F^2\right)_{\max} \tag{6}$$

where $\|\omega\|_F^2$ is the Frobenius norm of the rotation rate tensor. $\|D\|_F^2$ is the Frobenius norm of the strain rate tensor. ε stands for a positive small quantity, and an error occurs in order to prevent the phenomenon of the denominator being 0.

Vortex identification within the discharge passage of the inclined pump system was conducted using the Omega criterion (Ω = 0.70), with Figure 14 depicting the distributions of vortex structures under different exit setting angles. There exists a high-speed vortex at the entry region of the discharge conduit. Except for the β = 90° scheme, where the vortex structure exhibits significantly larger scale, all other angular configurations demonstrate relatively smaller vortex scales. Apart from the inlet of the outlet passage, the vortex structures are mainly located in front of the middle pier, with a small amount entering both openings. For schemes with the exit setting angles of 90° and 105°, the vortex structures in front of the partition pier are larger than those of other schemes and exhibit a spiral shape, indicating that the vortices at this location are relatively strong. For the exit setting angle schemes of 97.5° and 100°, the overall scale of the vortex structures is smaller, and they appear in a strip-like form within the left opening, which is due to the small flow inertia at this position. After a comprehensive comparison of the vortex structure distribution diagrams for the five schemes, it is observed that the vortex core distribution is the smallest when the angle is 97.5°. This corresponds with the smallest flow difference between the two openings at the angle of 97.5°.

3.4. Comparison of Pump System Performance Under Different Working Conditions

As demonstrated by the aforementioned analysis, the discharge flow rates through the two openings of the splitter pier in the outlet passage achieve near-identical values when the exit setting angle is set to 97.5°. Additionally, compared with other schemes, the outlet passage at an angle of 97.5° demonstrates superior performance in terms of hydraulic losses, internal flow patterns, and vortex structures. Therefore, the exit setting angle of 97.5 degrees was selected as the final optimization scheme.

While previous studies have predominantly focused on the pump's hydraulic performance at the design flow rate, actual operational conditions require operation across a range of flow rates. This paper, therefore, investigates the hydraulic performance of the optimized scheme under varying flow conditions. In order to facilitate the comparison, numerical simulation calculations were also performed for the original scheme. The performance curves for both the original and optimized pump designs at different flow rates are presented in Figure 15. The error bars in the figure are plotted based on the calculation error of the pump system efficiency under the optimal operating condition.

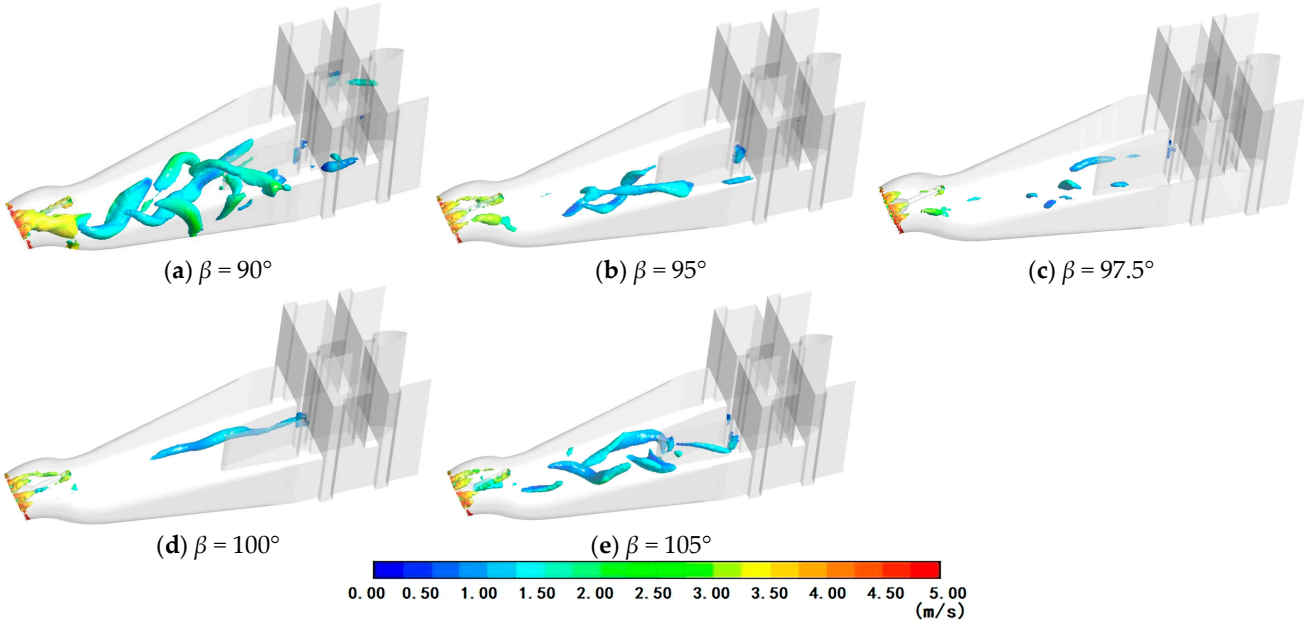


Figure 14. Vortex structure in the outlet passage under different schemes of exit setting angles.

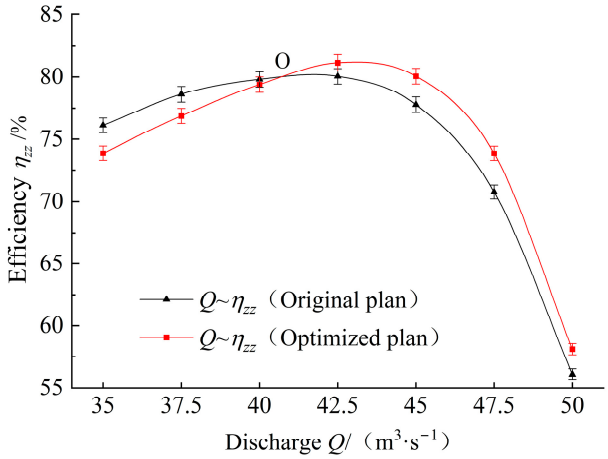


Figure 15. Comparison chart of the discharge efficiency between the original plan and the optimized plan.

The red curve in Figure 15 represents the efficiency curve of the optimized scheme pump system, while the black curve represents the original scheme. The two curves intersect at point O. The hydraulic performance of the optimized pump configuration does not surpass that of the baseline design across all flow conditions. Specifically, to the left of point O, the original scheme demonstrates higher efficiency than the optimized scheme. To the right of point O, the optimized pump scheme demonstrates higher efficiency than the original scheme. The D-value of efficiency initially increases with flow rate and subsequently diminishes, indicating reduced sensitivity of hydraulic performance to exit setting angle variations under high-flow conditions. The optimized scheme's guide vane exit setting angle of 97.5° is greater than that of the original scheme, and there is a certain flow deflection angle. As the flow rate decreases, the pressure on the back side of the guide vane outlet also decreases. Although the circulation at the guide vane exit of the optimized design remains small under low flow conditions, the combined effects of high velocity and pressure gradients at the exit cross-section [23], along with multiple bends in the outlet passage of the inclined pump system, lead to flow deterioration characterized by massive vortex generation, resulting in a sudden increase in hydraulic losses in the outlet passage.

This provides a robust explanation for the reduced efficiency of the optimized pump system compared to the original scheme under low-flow conditions.

Figure 16 shows the variation patterns of the deviation flow coefficients for the original and optimized schemes under different flow rates. As shown in the figure, the bias flow coefficient for the original scheme is greater than 1 under all flow conditions, and it generally shows an overall trend of initial reduction followed by subsequent increase. The original scheme shows that the flow rate through the left opening consistently exceeds that through the right one across all tested flow conditions. When it comes to 40 m^3/s, the flow rates in the left and right openings are closest to each other. The optimized scheme demonstrates a decreasing trend in bias flow coefficient as the flow rate increases. The coefficient is greater than 1 when the flow rate is less than 42.5 m^3/s, indicating that the right opening exhibits a lower flow rate compared to the left one. When the flow rate is greater than 45 m^3/s, the bias flow coefficient is less than 1, indicating that the left opening exhibits a lower flow rate compared to the right one. According to the velocity triangle of the impeller blade outlet of the axial flow pump, the tangential velocity of the outlet passage decreases as the flow discharge increases. Under the condition of large flow discharge, the water flows smoothly and directly into the guide vane body. Under the influence of the outlet angle of the guide blades in the improved scheme, the water flows more towards the right hole of the outlet passage, and the bias coefficient is less than 1. Under low flow conditions, the deviation flow in the optimized scheme is more severe than in the original scheme. Conversely, under high-flow conditions, the original scheme exhibits more pronounced flow deviation.

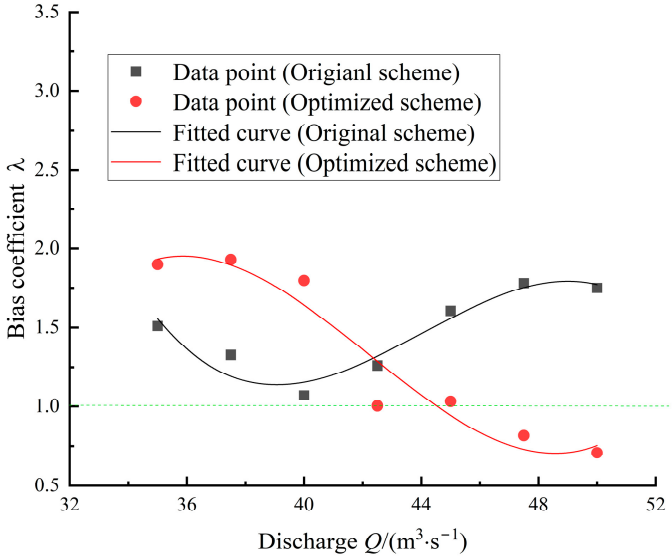


Figure 16. Bias coefficient of the original plan and the optimized plan under different flow conditions.

Figure 17 shows the curves of hydraulic loss variation at certain locations for the original and optimized schemes when discharge increases from 32 m^3/s to 52 m^3/s. In the optimized scheme, the guide vane's hydraulic loss is labeled as I; the outlet passage's hydraulic loss of the optimized scheme is labeled as II; III represents the sum of hydraulic losses from the aforementioned two components under the optimized scheme. Similarly, in the original scheme, the guide vane's hydraulic loss is labeled as 1; the outlet passage's hydraulic loss of the original scheme is labeled as 2; 3 represents the sum of hydraulic losses from the aforementioned two components under the optimized scheme.

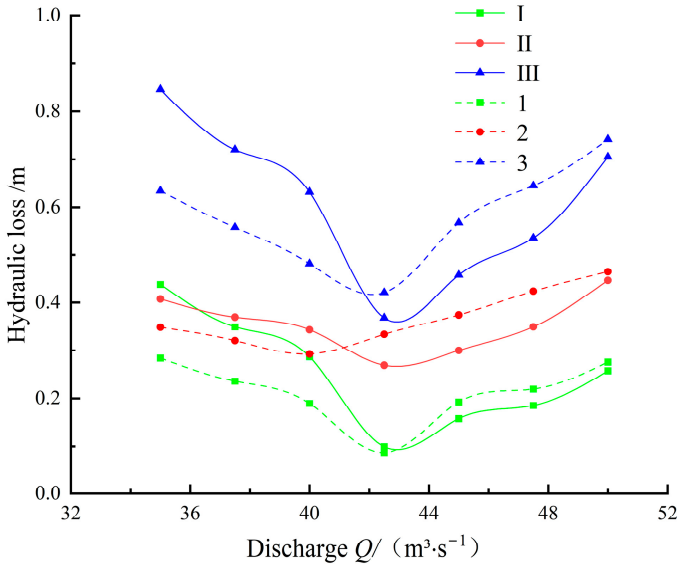


Figure 17. Hydraulic losses of guide vane and outlet passage under different flow conditions.

Since the inlet passage and the impeller chamber are identical in both the original and optimized schemes, the main factors affecting the pump system's hydraulic performance are primarily the guide vane and the outlet passage. As evidenced by Figure 17, under low-flow conditions, the optimized scheme exhibits higher hydraulic loss in both the guide vane and discharge passage compared to the original scheme. Conversely, when the discharge becomes higher, the guide vane loss and the outlet passage loss of the optimized scheme are both less than those of the original scheme. The combined hydraulic losses of the outlet passage and the guide vane for both the original and optimized schemes follow the same pattern, which is consistent with the variation pattern of the bias flow coefficients mentioned earlier.

By examining the efficiency changes of the original and optimized schemes under various discharges, it is observed that the severity of the deviation in flow affects the performance of the whole pump system. Under identical conditions, the further the bias coefficient is from 1, the greater the relative difference in flow rates between the two openings, and consequently, the lower the performance is.

The comparison of internal streamlines in the outlet passage between the original and optimized schemes under certain flow conditions is shown in Figure 18. As evidenced by the streamline diagram, when the flow rate is low, the streamlines of the left hole in both the original and optimized schemes are relatively smooth, while the streamlines of the right hole are disordered with local vortices. The degree of disorder in the right hole of the optimized scheme is greater than that in the left hole. For the optimized scheme, at high flow rates, the flow patterns in both openings are similar, with the presence of small localized vortices, which is consistent with the information reflected in the bias coefficient graph.

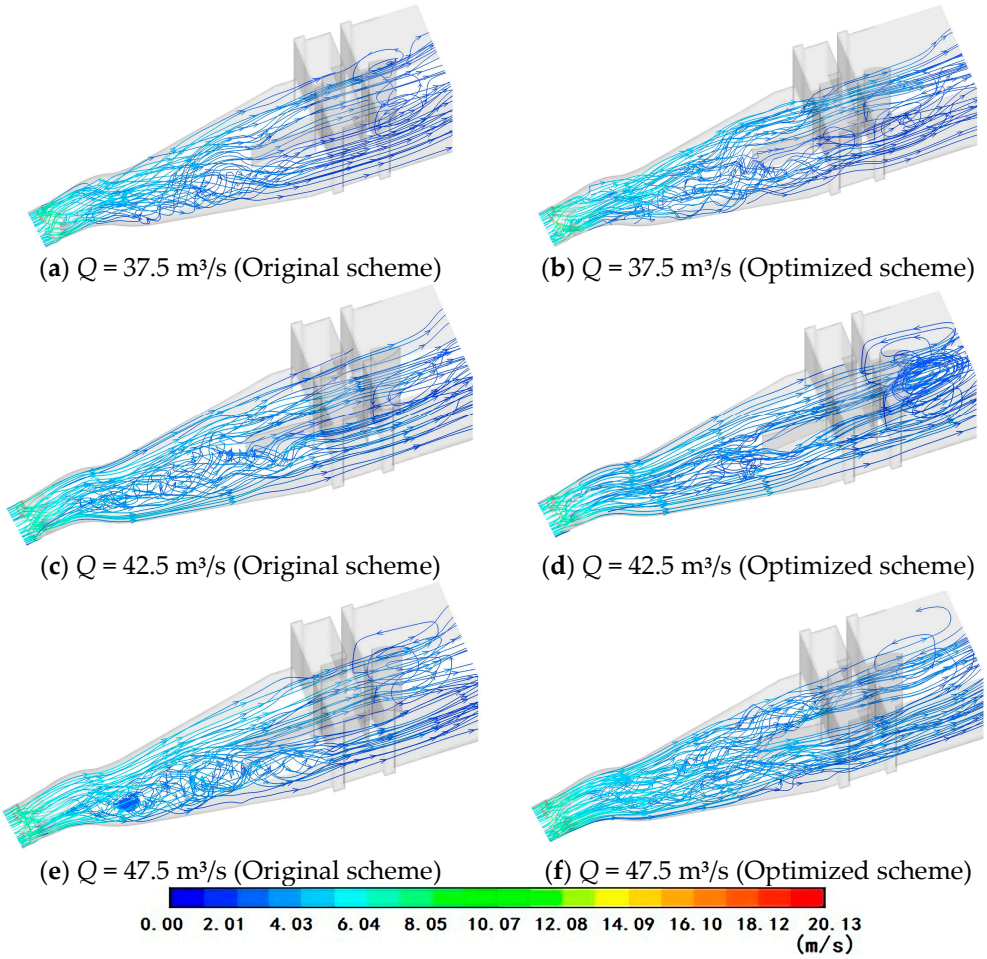


Figure 18. Flow trace diagram of guide vane and outlet passage for the original scheme and the optimized scheme.

In a certain slanted axial flow pumping station that did not adopt the diversion improvement measures for the outlet passage, the working gate vibrated during the operation of the pump system. According to the research results, the bias flow in the outlet passage is severe. The left hole has a large flow rate while the right hole has a smaller flow rate. The water flow in the left hole is smooth, while there is a large range of vortex zones in the right hole. As shown in the original scheme flow field (Figure 18a,c,e), due to the large range of vortex zones in the right hole, the suspended working gate will be prone to unstable vibration under the action of water flow. When the flow state in the slanted outlet passage was improved (Figure 18b,d,f), the water flow in the left and right holes of the outlet passage will be smooth, and there are basically no vortices in both holes. The water flows smoothly below the working gate, which is conducive to improving the operational stability.

4. Conclusions

Based on the numerical simulation method validated by pump system model tests, three-dimensional turbulent flow numerical simulations were conducted for the slanted axial-flow pump system with guide vane exit setting angles ranging from 90° to 105°. The results were analyzed to determine the impact patterns of the exit setting angle on the internal flow within the outlet passage and the guide vane, as well as on hydraulic performance indicators such as hydraulic loss and pump system efficiency. The conclusions are as follows:

When conventional guide vane exit setting angles are used in the slanted axial-flow pump system, there is a severe deviation in flow within the outlet passage. Under the design flow condition, the flow rates through the left and right openings of the outlet passage differ significantly, with an outlet passage bias coefficient $\lambda = 1.606$. The main flow through the passage is biased towards the left opening, and there is a large vortex area in the right opening.

As the exit setting angle increases, the flow field in the upstream section of the guide vane remains essentially the same, and the area of the low-velocity zone at the guide vane outlet exhibits a trend that first decreases and then increases.

With the increase of the exit setting angle, looking in the direction of the water flow, the outlet passage's main flow gradually shifts from the left opening to the right opening. When the angle is 97.5°, the flow rates in two openings of the outlet passage become nearly equal, the bias flow coefficient also reaches near 1, thereby effectively eliminating the deviation flow.

The head loss in the outlet passage of the slanted axial-flow pump system is greatly influenced by the bias flow coefficient. As the bias flow coefficient approaches 1, the head loss in the outlet passage reduces to the minimum value accordingly. At the design condition with a guide vane exit setting angle of 97.5°, the outlet passage's head loss reduces to its minimum of 0.230 m.

With regard to the slanted axial flow pump system, modifying the guide vane exit setting angle can effectively ameliorate the deviation flow within the outlet passage, improve the outlet passage's flow condition, reduce the hydraulic loss in the outlet passage, and enhance the whole pump system's efficiency. The research outcomes can offer technical support for the hydraulic design of analogous pump systems. For the problem of biased flow in the outlet passage of a slanted pump system, further research can be conducted from aspects such as unsteady flow, changing the blade angle or the speed of the pump, and the impact of altered flow conditions on the stability of the working gate.

Author Contributions: L.X.: Writing—original draft, Writing—review and editing, Visualization, Validation. L.C.: Writing—original draft, Methodology, Investigation. B.Z.: Data curation, Supervision. H.Z.: Resources, Data curation. T.J.: Conceptualization. H.D.: Formal Analysis. C.Q.: Visualization. All authors have read and agreed to the published version of the manuscript.

Funding: This research was funded by Jiangsu Water Conservancy Science and Technology Project grant number 2022010 and the Jiangsu South-to-North Water Diversion Technology R&D Project grant number JSNSBD202105.

Data Availability Statement: All data generated or analyzed during this study are included in this published article.

Conflicts of Interest: Author Hucheng Zhang was employed by the Yangzhou Survey Design Research Institute Co., Ltd. The remaining authors declare that the research was conducted in the absence of any commercial or financial relationships that could be construed as a potential conflict of interest.

References

1. Gao, P.L. South-to-north water diversion and slanted axial flow pump. *Gen. Mach.* **2003**, *2*, 51–53.
2. Voith Hydro Holding GmbH & Co., KG. Pumps Tailormade Solutions for Water Applications. Available online: https://voith.com/corp-de/12_06_Pumpenbroschuere.pdf (accessed on 5 March 2025).
3. Zhang, R.; Chen, H.X. Numerical analysis of cavitation within slanted axial flow pump. *J. Hydrodyn.* **2013**, *25*, 663–672. [CrossRef]
4. Pan, Z.J.; Xu, L.; Shen, X.Y.; Hong, F.; Zhang, H. Conduit hydraulic optimization of slanted pump system for Babao Pumping Station of Hangzhou. *J. Drain. Irrig. Mach. Eng.* **2018**, *36*, 501–508.
5. Chen, S.H.; Zhou, Z.F.; He, Z.N.; Liu, R.G.; Xue, F.J.; Lian, S.J. Numerical simulation of flows in 30° slanting inlet duct and model test of pump set. *J. Hydrol. Eng.* **2012**, *31*, 204–208, 216.

6. Wang, L.; Chen, S.S.; Zhou, Z.F.; Li, T.J. Analysis and test for flow characteristics of 45° slanting axial flow pumping system. *J. Water Resour. Archit. Eng.* **2013**, *11*, 149–152.
7. Chen, Y.L.; Hua, M.; Cao, G.H. Hydraulic model test of inclined axial flow pump station at 30° angle. *Hydrol. Sci. Eng.* **2000**, *2*, 55–58.
8. Zhang, J.G.; Liu, M.Q.; Liang, X.; Zhang, H.B. Simulation of Flow Pattern in the Inflow Conduit of Sujiaji Pumping Station. *J. Drain. Irrig. Mach. Eng.* **2005**, *6*, 19–22.
9. Liu, R.G.; Ma, X.Z.; Zhan, L. Model Test Study of 30° Slanted Axial-flow Pump Set in Huangjiaba. *Chin. Rur. Wat. Hydrop.* **2016**, *2*, 109–111.
10. Hu, W.Z.; Tong, D.B.; Li, Z.B.; Wang, R.; Yang, F. Numerical Analysis of Internal Flow in a Slanted Axial-flow Pump. *J. Irrig. Drain.* **2021**, *40*, 66–72.
11. Yang, R.D.; Mo, W.Z.; Zhang, H.P. Hydraulic Model Development for 30° Axis Pump Unit with Application Analysis. *Pump. Technol.* **1997**, *5*, 3–7.
12. Yan, S.K. Study on Water Bias Problem in Outlet Passage of the Large Pumping System with Slanting and Extensive Pump Shaft. Master's Thesis, Yangzhou University, Yangzhou, China, 2019.
13. Chen, Y.L.; Sun, Q.; Li, Z.X.; Gong, Y.; Zhai, J.W.; Chen, H.X. Numerical study on the energy performance of an axial-flow pump with different wall roughness. *Front. Energy Res.* **2022**, *10*, 943289. [CrossRef]
14. He, Z.N.; Zhou, Z.F.; Tan, Q.; Jiang, H.M.; Yuan, J.B.; Chen, S.S. Characteristic test of 15° slanting axis pump set. *Drain. Irrig. Mach. Eng.* **2008**, *26*, 36–40, 54.
15. Xie, L.H.; Wang, F.J.; He, C.L.; Su, S.L.; Zhang, S.C.; Wang, B.L. Experimental investigation on hydrodynamic characteristics of a 15 degree slanted axial flow pump system. *J. Hydraul. Eng.* **2019**, *50*, 798–805.
16. Tong, Z.M.; Yang, Z.Q.; Tong, S.G.; Shu, Z.K.; Cao, X.K.E. Investigating the hydraulic performance of slanted axial flow pumps using an enstrophy dissipation-based hybrid optimization approach. *Phys. Fluids.* **2023**, *35*, 057117. [CrossRef]
17. Fei, Z.D.; Xu, H.; Zhang, R.; Zheng, Y.; Mu, T.; Chen, Y.H. Numerical simulation on hydraulic performance and tip leakage vortex of a slanted axial flow pump with different blade angles. *Proc. Inst. Mech. Eng. Part C J. Mech. Eng. Sci.* **2022**, *236*, 2775–2790. [CrossRef]
18. Lu, L.G.; Liu, L.J.; Liu, J. Analysis of flow pattern in outlet conduit of pumping station. *J. Hydraul. Eng.* **2000**, *3*, 71–78.
19. Xu, L.; Xia, B.; Shi, W.; Liu, J.; Yan, S.K.; Lu, L.G. Influence of middle pier lengths on hydraulic characteristic of outlet conduit in pump system with slanted extension shaft. *Trans. Chin. Soc. Agric. Eng.* **2020**, *36*, 74–81.
20. Xu, L.; Huang, G.H.; Shi, W.; Yan, S.K.; Xia, B.; Lu, W.G. Influence of guide plate on hydraulic performance of outlet conduit in large-scale slanted pump system. *Chin. J. Hydrodyn.* **2020**, *35*, 479–487.
21. Wang, B.H.; Wang, F.J.; Xie, L.H.; Wang, C.Y.; Su, S.L.; Zhu, Q.R. Flow deviation in the discharge passage of a slanted axial flow pump system. *J. Hydraul. Eng.* **2021**, *52*, 829–840.
22. Shi, L.J.; Chai, Y.; Wang, L.; Xu, T.; Jiang, Y.H.; Xing, J.; Yan, B.Y.; Chen, Y.Y.; Han, Y. Numerical simulation and model test of the influence of guide vane angle on the performance of axial flow pump. *Phys. Fluids* **2023**, *35*, 015129. [CrossRef]
23. Song, X.J.; Liu, C. Experimental investigation of floor-attached vortex effects on the pressure pulsation at the bottom of the axial flow pump sump. *Renew. Energy* **2020**, *145*, 2327–2336. [CrossRef]
24. Wang, K. Iterative schemes for the non-homogeneous Navier-Stokes equations based on the finite element approximation. *Comput. Math. Appl.* **2016**, *71*, 120–132. [CrossRef]
25. Launder, B.E.; Spalding, D.B. The numerical computation of turbulent flows. *Comput. Meth. Appl. Mech. Eng.* **1974**, *3*, 269–289. [CrossRef]
26. Gong, C.Y.; Zeng, Y.L.; Li, R.N.; Ma, X.J. An analysis of the flow pattern character of pumping station forebay before and after reconstruction and research on energy conservation and consumption reduction. *Chin. Rur. Wat. Hydrop.* **2022**, *5*, 87–94+100.
27. Bei Fang Investigation, Design & Research Co., Ltd. *Expand the Model Test Report of the Pump System of Hangzhou Babao Drainage Pumping Station in Hangzhou Babao Drainage Pumping Station in Hangjia Lake South, Tianjing, China*; Bei Fang Investigation, Design & Research Co., Ltd.: Tianjin, China, 2018.
28. Guan, X.F.; Yang, J.J. Benchmark Testing Review of Pump Models in China's SNWDP: A Ministry of Water Resources Perspective. *Chin. Rur. Wat. Hydrop.* **2006**, *2*, 123–126.
29. Shi, L.J.; Tang, F.P.; Zhou, H.L.; Tu, L.L.; Xie, R.S. Axial-Flow pump hydraulic analysis and experiment under different swept-angles of guide vane. *Trans. Chin. Soc. Agric.* **2015**, *31*, 90–95.
30. Zhao, Z.L.; Qian, Z.D.; Guo, Z.W. Experimental Study on the Effect of Rear Guide Vane Angle Adjustment on Axial-Flow Pump Performance. In Proceedings of the 11th National Conference on Hydraulic Machinery and Systems, Beijing, China, 19 October 2018; pp. 129–136.
31. Qiu, B.Y.; Yuan, W.S. Analysis of hydraulic loss of outlet channel of axial flow pump and design of rear guide vane without outlet ring. *J. Hydro. Eng.* **1993**, *4*, 70–75.

32. Shi, L.J. Research on Optimization Design Method and the Key Technology of the Axial Flow Pump Hydraulic Model. Ph.D. Thesis, Yangzhou University, Yangzhou, China, 2017.
33. Liu, C.Q.; Wang, Y.Q.; Yang, Y.; Duan, Z.W. New omega vortex identification method. *Sci. China Phys. Mech. Astron.* **2016**, *59*, 684711. [CrossRef]

Disclaimer/Publisher's Note: The statements, opinions and data contained in all publications are solely those of the individual author(s) and contributor(s) and not of MDPI and/or the editor(s). MDPI and/or the editor(s) disclaim responsibility for any injury to people or property resulting from any ideas, methods, instructions or products referred to in the content.